Micromagnetic modelling of magnetostriction under uniaxial stress

Inna Lobanova, Stéphane Despréaux, Stéphane Labbé, Carola Celada-Casero, Frenk van den Berg

Micromagnetic modelling of magnetostriction under uniaxial stress

I.I. Lobanova[a,b,*], S. Despréaux[b], S. Labbé[c], C. Celada-Casero[d,e], F. van den Berg[e]

[a] *Université Grenoble Alpes, LJK, 38000 Grenoble, France*
[b] *Laboratoire Jean Kuntzmann, CNRS, 38000 Grenoble, France*
[c] *Sorbonne Université, CNRS, Université de Paris, Laboratoire Jacques-Louis Lions (LJLL), F-75005 Paris, France*
[d] *National Centre for Metallurgical Research (CENIM-CSIC), E-28040 Madrid, Spain*
[e] *Tata Steel, 1970CA IJmuiden, Netherlands*

Abstract

In the current work we present the results of 3D micromagnetic modelling of magnetostrictive strain and magnetic hysteresis under uniaxial stress in ferrite. The simulations are performed on artificial microstructures with different grain orientations that allow to take into account the anisotropy of magnetic and mechanical properties of iron-based alloys. The obtained results are in reasonable agreement with experimental observations. The proposed method opens a path to predictive modelling of the magnetic properties of different textured steels in the context of in-line non-destructive testing.

1. Introduction

During the process of magnetization ferromagnetic materials undergo changes in their shape or dimensions due to the coupling of magnetic order and strain. In particular, as the magnetization goes up, the magnetostrictive strain increases with magnetic field before reaching a saturating value, λ [1]. This effect causes energy loss due to frictional heating in susceptible ferromagnetic cores. The effect is also responsible for the low-pitched humming sound that can be heard coming from transformers, where oscillating AC currents produce a changing magnetic field. The reciprocal effect, the change of the magnetic susceptibility in response to an applied field of a material when subjected to a mechanical stress, is called the Villari effect. Thus the mechanical stresses strongly influence the magnetic properties of ferromagnetic steel, affecting especially the hysteresis [2–5]. Therefore the development of appropriate simulation tools is of particular interest for industrials to optimize the material conception.

The micromagnetic theory [6] is a powerful tool to describe the non-linear behaviour of ferromagnetic media. Although the micromagnetic modelling of magnetization process and domain structure are now well mastered, the description of magnetostriction and associated magneto-mechanic interactions remains unachieved or badly implemented in the literature [7]. Indeed the modelling of the intrinsic stress due to a free strain like magnetostriction is rather complex and therefore the mechanical approach to this problem is relevant. In this paper, we will address the development of a 3D stress dependent micromagnetic model that takes into account the magneto-mechanical coupling. When the magnetic materials are subjected to an applied stress, the induced magneto-elastic energy must be taken into account in the Gibbs free energy. The modelling is therefore achieved by introducing elastic and magneto-elastic interactions depending on stress and magnetization in the free energy expression [8, 9].

The variation of magnetostrictive strain is linked to the domain wall movement and magnetization reversal process, which are usually complex phenomena that depend on the microstructure of magnetic material [2, 3, 10]. In the present simulations, we have considered the effect of uniaxial stress on the magnetic hysteresis in ferrite with different grain orientations. This ferromagnetic material displays anisotropy of magnetic, magnetostrictive and elastic properties, and therefore the modelling of magnetic properties of different microstructures can help to shed more light on the influence of applied stress and predict its effect on the magnetic properties of the material.

2. Method

Micromagnetics and domain theory are based on the same variational principle which is derived from thermodynamic principles, as established initially by Landau and Lifshitz in [11] and reviewed in [6] and [12]. According to this principle, the vector field of magnetization directions $\mathbf{m} = \mathbf{M}/M_s$ is chosen so that the total free energy reaches an absolute or relative minimum under the constraint $|\mathbf{m}| = 1$, where $\mathbf{M}$ is the magnetization vector and M_s is the value of magnetization at saturation. In the initial micromagnetic model, the Landau-Lifshitz (LL) equation allows to predict the evolution of magnetization

*Corresponding author
Email address: inna.lobanova@univ-grenoble-alpes.fr (I.I. Lobanova)

that depends on a combination of purely magnetic excitations by external magnetic, crystalline anisotropy, ferromagnetic exchange, and demagnetization fields [6]. In our model we have incorporated the internal elastic and magnetic stresses into the additional magnetostrictive excitation field and its contribution to the free energy [8]. The sum of all energies corresponding to these fields gives:

$$E_{tot}(\mathbf{M}) = E_{ex} + E_{ani} + E_{Zeeman} + E_{demag} + E_{m-el}. \quad (1)$$

The exchange energy term favours a homogeneous magnetic state such that any gradient of the local magnetization leads to an increase in E_{ex},

$$E_{ex} = A \int_V (\nabla \mathbf{m})^2 \, dV, \quad (2)$$

where A is the exchange stiffness constant.

The energy of a ferromagnet that depends on the direction of the magnetization relative to the structural axes of the material is expressed as

$$E_{ani} = \int_V \Phi(\mathbf{M}) dV, \quad (3)$$

where $\Phi(\mathbf{M})$ is the anisotropy energy density whose expression verifies $\Phi(\mathbf{M}) = K_1(\alpha^2\beta^2+\beta^2\gamma^2+\gamma^2\alpha^2)+K_2\alpha^2\beta^2\gamma^2$ in a cubic crystal. Here K_1, K_2 are the anisotropy constants, α, β and γ are directional cosines ($\mathbf{M} = M_s(\alpha, \beta, \gamma)$).

The interaction energy of the magnetization vector field with an external field H_{ext} (so called Zeeman energy) is simply:

$$E_{Zeeman} = -\mu_0 \int_V \mathbf{H_{ext}} \cdot \mathbf{M} \, dV, \quad (4)$$

where $\mathbf{H_{ext}}$ is the external magnetic field.

The stray field magnetic energy tends to demagnetize the material and is expressed as

$$E_d = -\frac{\mu_0}{2} \int_V \mathbf{H_d} \cdot \mathbf{M} \, dV, \quad (5)$$

where $\mathbf{H_d}$ is the demagnetizing magnetic field.

And finally, the magneto-elastic energy is the sum of external and intrinsic stress contributions that depend on the magnetization $\mathbf{M}$ and the mechanical displacement field $\mathbf{u}$:

$$E_{m-el} = \int_V \lambda^m : [\mathbb{C} : \varepsilon(\mathbf{u}) - \mathbb{C} : (\lambda^m : \mathbf{m} \otimes \mathbf{m})].\mathbf{m} dV, \quad (6)$$

where $\mathbb{C}$ is the elastic constants tensor, $\varepsilon(\mathbf{u})$ is the mechanical deformation as a function of the displacement field $\mathbf{u}$, λ^m is the magnetostriction constants tensor.

The basic problem consists in minimizing the total free energy (1) and finding the equilibrium magnetization at each value of the external magnetic field, which allows to derive the magnetic hysteretic behaviour [6]. The computation of the equilibrium magnetization state is based on solving the LL equation over time. The discretized time step is chosen in a way that minimizes the magnetic energy. The displacement field is computed by solving the mechanical equilibrium equation $\nabla(\mathbb{C} : \varepsilon(\mathbf{u})) = \nabla(\mathbb{C} : \lambda^m : \mathbf{m} \otimes \mathbf{m})$ with given material parameters, external magnetic field and equilibrium magnetization [7, 9].

The micromagnetic model described above has been implemented in a self-written software EMicroM by using specific numerical methods [13–15]. The problem is discretized using a Finite Volume Approximation which preserves the main properties of the operator given in the continuous model, i.e. positivity and symmetry. Furthermore, the discretization of the demagnetized operator leads to a block-Toeplitz structure for regular 3D cubic grid, which allows to build fast solving method for cubic domains.

3. Materials

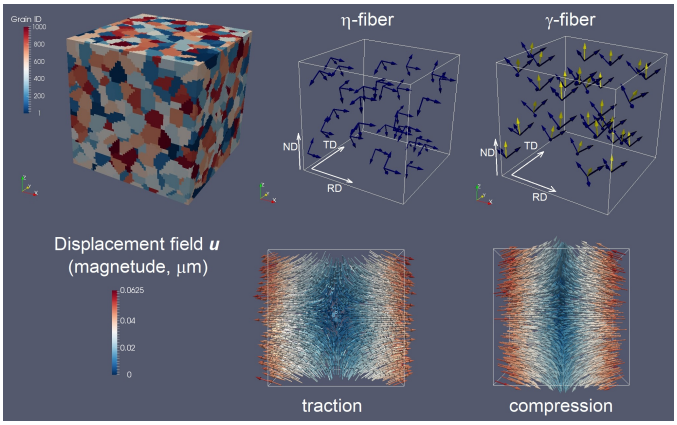

Figure 1: Top (from left to right): Example of grain distribution in a microstructure with 1000 grains. Each colour corresponds to the ID of each grain; Example of grain orientations in RVE coordinate system for η-fiber and γ-fiber. Dark blue vectors represent <100> family of directions, yellow is the [111] direction. Bottom: vector representation of the displacement field $\mathbf{u}$ distribution in case of traction and compression. The amplitude is given in μm.

The representative volume elements (RVE) in this study are cubes $100\times100\times100$ μm^3 with the resolution restricted to $64 \times 64 \times 64$ ($\sim$ 260 000) cubic cells, owing to the optimization of computing time. We performed computations on artificial 3D microstructures generated using multi-level Voronoi software developed by Tata Steel [16]. The material configuration files contains the information about Euler angles, that allows us to perform the rotation of crystals in reference to the RVE coordinate system. Here the X, Y and Z axes of cube correspond to rolling (RD), transverse (TD) and normal (ND) directions in steel sheets. The material parameters used for simulations are given in the Table 1, where M_s is the magnetization at saturation, A is the exchange stiffness constant, K_1, K_2 are the cubic magneto-crystalline anisotropy constants, λ_{100}, λ_{111}

Table 1: Material parameters (see text for details)

$M_s = 1.7\ MA/m$	$A = 18\ pJ/m$	$K_1 = 48\ kJ/m^3$
$K_2 = 0$	$\lambda_{100} = 21 \cdot 10^{-6}$	$\lambda_{111} = -21 \cdot 10^{-6}$
$C_{11} = 228\ GPa$	$C_{12} = 132\ GPa$	$C_{44} = 116.5\ GPa$

are the magnetostriction constants along [100] and [111] directions, and C_{11}, C_{12}, C_{44} are the elastic stiffness tensor components in Voigt notation. The external magnetic field and the uniaxial stress are both applied parallel to RD direction. The example of microstructure and stress field distribution u are given in the Fig. 1.

We have computed hysteresis curves for selected microstructures: non-oriented (random) and oriented grains (η- and γ-fibers). There are two random structures: with 8 grains (grain size $\sim 50\ \mu m$) and 1000 grains (grain size $\sim 13\ \mu m$). The oriented microstructures both have 1910 grains (grain size $\sim 10\ \mu m$) but the grains are rotated differently: η-fiber is characterised by <100> || RD and γ-fiber is characterised by <111> || ND.

4. Results and Discussion

The computed hysteresis curves under compressive and tensile uniaxial stresses for randomly oriented grains are displayed in the Fig. 2

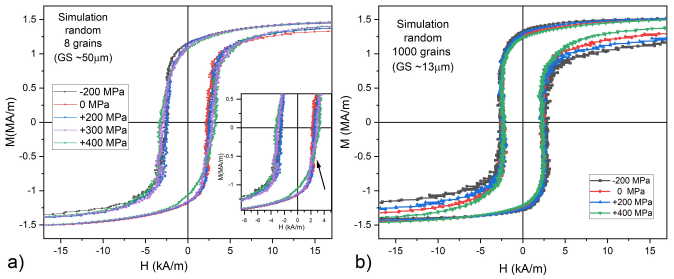

Figure 2: Hysteresis curves under uniaxial stress for random orientation of grains a) 8 grains; insert: zoom on the region where the curves cross; b) 1000 grains. The applied stress values are given in legend.

For 8 grains configuration the small number of grain orientation leads to a situation, where some of the grains has an easy-axis close to the applied field, and the tensile stress increases the anisotropy to favour the magnetisation vectors alignment with the external magnetic field. Therefore we observe that an increase of tensile stress leads to an increase of coercivity.

When we increase the number of grains to 1000, the dispersion of grain orientations becomes larger. The resulting

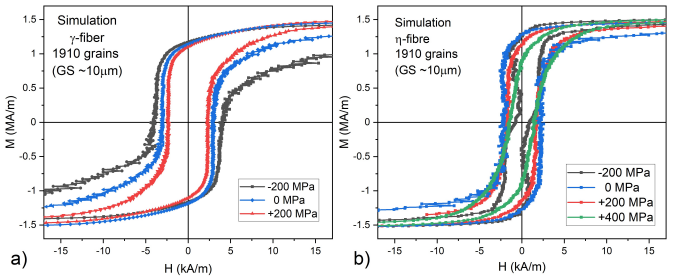

Figure 3: Hysteresis curves under uniaxial stress for a microstructure with 1910 grains (grain size $\sim 10\ \mu m$) and a) γ-fiber; b) η-fiber. The applied stress values are given in legend.

hysteresis curve is given in the Fig. 2b. Here we do not observe any significant influence of the stress on coercivity, however we see an increase in permeability with the increasing tensile stress (blue and green curves in the Fig. 2b) and a decrease with the compressive uniaxial stress (black curve in Fig. 2b).

The results of hysteresis simulation for grain-oriented microstructures are given in the Fig. 3. We can see that the resulting hysteresis curves show a strong dependence of the properties on the texture. This confirms that our simulation software takes well into account the orientation of grains and the anisotropy of magnetic and elastic properties of the material.

For γ-fiber we observe a strong increase in coercivity with the compressive stress and an increase in permeability for the tensile stress that agrees well with predictions for this texture. For η-fiber increasing tensile stress leads to a decrease of coercive field, however it is still higher than in case of compression. This is due to the fact that for this virtual microstructure the <100> direction is strictly parallel to RD and therefore there is always one easy-axis parallel to RD, and two easy axes in a plane perpendicular

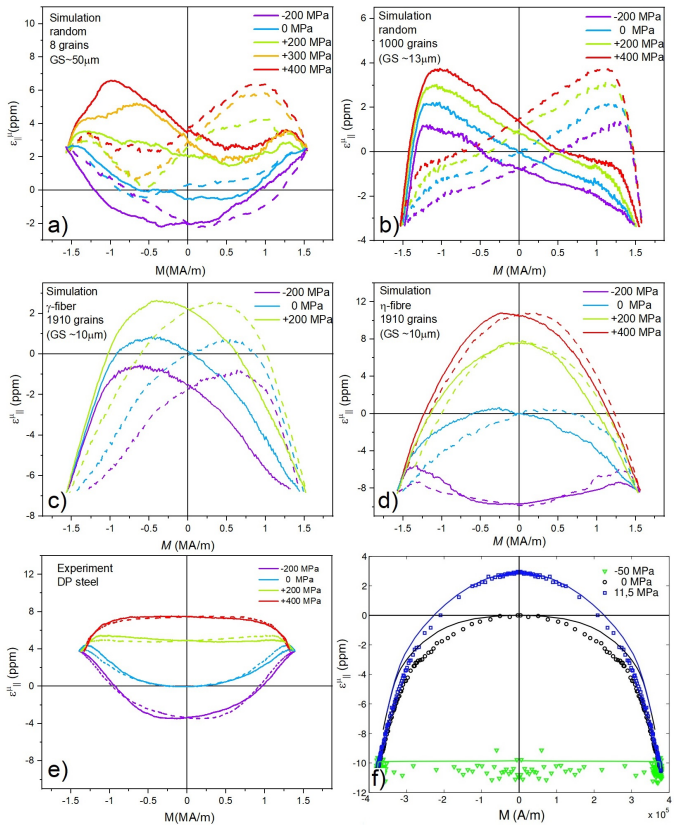

Figure 4: (a)-(d) Simulated longitudinal magnetostriction strain as a function of magnetization for a) randomly oriented 8 grains ; b) randomly oriented 1000 grains ; c) γ-fiber 1910 grains ; d) η-fiber 1910 grains. Solid lines correspond to the field sweep up, and dashed line - the field sweep down. (e)-(f) Experimentally measured longitudinal magnetostriction strain as a function of magnetization for e) DP steel ; f) ferrite NiZn (ahysteretic) [4]. Stress values are given in legends.

to RD. In this situation there are multiple possibilities to minimize the energy, which have an impact on the computed results. This obstacle can be overcome by averaging the calculation result over multiple microstructures.

We would like to note that the values of H_c are much higher than those of bulk iron. This can be explain by the microscopic size of the modelled microstructures as well as an insufficient number of degrees of freedom for magnetization rotations due to the limited number of computational cells. The authors continue to work on the parallelisation of the computation to overcome this obstacle.

The presented model allows to calculate the average magnetostrictive strain in the material as an equivalent elastic strain. The results for the longitudinal magnetostrictive strain $\varepsilon^{\mu}_{||}$ as a function of the magnetisation M are presented in the Fig. 4.

The behaviour of the magnetostriction corresponds well to that observed experimentally [4, 17]. The sign of the strain at the saturation is in coherence with crystallographic orientations of grains in the considered microstructures. The tensile stress increases the longitudinal magnetostrictive strain $\varepsilon^{\mu}_{||}$, and, in the case of the non-oriented grains, shifts the maximum to lower magnetization values, whereas the compressive stress decreases $\varepsilon^{\mu}_{||}$.

It is interesting that magnetostriction behaviour of simulated η-fiber shows similarity to the experimental measurements for DP steel. We also see the similarities in the hysteresis for tensile stress (see Fig.5). Even though, the reason for this similarity is not evident because of the different microstructures of the 2 steel grades, this shows that the modelling of magnetostriction under uniaxial stress reflects well the hysteresis behaviour and is very sensitive to the microstructure.

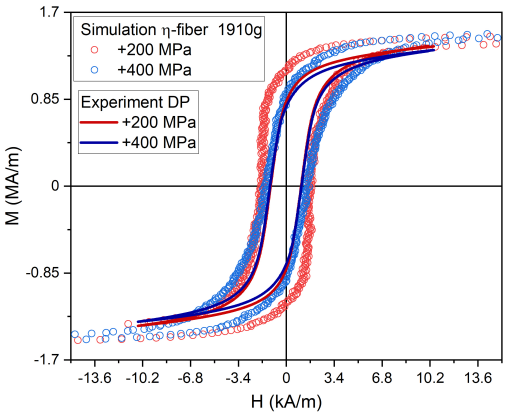

Figure 5: Comparison between the simulated hysteresis curves for η-fiber and the experimentally measured ones for DP steel [5]

5. Conclusions

The micromagnetic modelling of magnetostriction under uniaxial stress for different grain orientations has been carried out by including the magneto-elastic energy term in the Landau–Lifshitz equation. The computed magnetization curves display a change in the shape of hysteresis loops and the magnetic properties e.g., coercivity and remanence, under the applied stress in a manner which is in reasonable agreement with the reported experimental results of others. The magnetostriction as a function of magnetization follows well the characteristics of considered microstructures and applied uniaxial stress. The obtained results give a solid base for further development of the modelling algorithms as well as computational capacities.

6. Acknowledgements

The authors are grateful to Prof. O. Hubert from ENSPSay for provided experimental data of hysteresis and magnetostrictive strain in DP steel. This work has been developed within the project "Online Microstructure Analytics" (Ref. OMA, Grant Agreement No. 847296) that has received funding from the Research Fund for Coal and Steel of the European Union, which is gratefully acknowledged. This work was performed using HPC resources from GENCI-IDRIS (Grant 2022-AD010913441) and GRICAD infrastructure.

References

[1] J.P.Jules, On the effects of magnetism upon the dimensions of iron and steel bars, Phil. Mag. and J. of Sci. 3 (1847) 76–87.
[2] D. Singh, P. Rasilo, F. Martin, A. Belahcen, A. Arkkio, Effect of mechanical stress on excess loss of electrical steel sheets, IEEE Trans. Magn. 51 (2015) 1001204.
[3] U.Aydin, P. Rasilo, F. Martin, A. Belahcen, L. Daniel, A. Haavisto, A. Arkkio, Effect of multi-axial stress on iron losses of electrical steel sheets, JMMM 469 (2019) 19–27.
[4] L.Daniel, O.Hubert, B.Vieille, Multiscale strategy for the determination of magneto-elastic behaviour: discussion and application to Ni-Zn ferrites, Int. Jour. of Appl. El. and Mec. 25 (2007) 31–36.
[5] A.Ouaddia, O.Hubert, J.Furtado, D. Gary, S. Depeyre, Piezomagnetic behavior: experimental observations and multiscale modeling, Mechanics & Industry 20 (2020) 1–11.
[6] W. Brown Jr., Micromagnetics, Vol. 18, John Wiley and Sons, Inc., 1963, p. 153.
[7] Y. C. Shu, M. P. Lin, K. C. Wu, Micromagnetic modeling of magnetostrictive materials under intrinsic stress, Mech. of Mat. 36 (2004) 975–997.
[8] G.Carbou, M.A.Efendiev, P.Fabrie, Global weak solutions for the Landau–Lifschitz equation with magnetostriction, Math. Meth. Appl. Sci. 34 (2011) 1274–1288.
[9] F. S. Mballa-Mballa, O. Hubert, S. He, S. Depeyre, P. Meilland, Micromagnetic modeling of magneto-mechanical behavior, IEEE Trans. Mag. 50 (2014) 1–4.
[10] A. Hubert, R.Schaefer, Magnetic domains: the analysis of magnetic microstructures, Springer-Verlag Berlin Heidelberg, 2009, p. 686.
[11] L. Landau, E. Lifshitz, On the theory of the dispersion of magnetic permeability in ferromagnetic bodies, Phys. Z. Sowjetunion 8 (1935) 153–169.
[12] W. Döring, Handbuch der Physik: Mikromagnetismus, Vol. 18/2, Springer, Berlin, Heidelberg, New York, 1966, p. 341–437.
[13] S.Labbe, Numerical simulation of high-frequency behaviour of ferromagnetic materials. PhD thesis. (1998).
[14] S.Labbe, P.Leca, Fast solution of quasi-stationary maxwell equations: multi-level toeplitz matrices. application to micromagnerism, C. R. Acad. Sci. Paris 327 (1998) 415–420.
[15] S.Labbe, Fast computation for large magnetostatic systems adapted for micromagnetism, SIAM J. SCI. COMPUT. 26 (2005) 2160–2175.

[16] P. Kok, W. Spanjer, H. Vegter, A microstructure based model for the mechanical behavior of multiphase steels, KEM 651-653 (2015) 975–980.
[17] O.Hubert, Multiscale magneto-elastic modeling of magnetic materials including isotropic second order stress effect, JMMM 491 (2019) 165564.